

# A Structural Molar Volume Model for Oxide Melts Part III: Fe Oxide-Containing Melts



ERIC THIBODEAU, AIMEN E. GHERIBI, and IN-HO JUNG

As part III of this series, the model is extended to iron oxide-containing melts. All available experimental data in the FeO-Fe<sub>2</sub>O<sub>3</sub>-Na<sub>2</sub>O-K<sub>2</sub>O-MgO-CaO-MnO-Al<sub>2</sub>O<sub>3</sub>-SiO<sub>2</sub> system were critically evaluated based on the experimental condition. The variations of FeO and Fe<sub>2</sub>O<sub>3</sub> in the melts were taken into account by using FactSage to calculate the Fe<sup>2+</sup>/Fe<sup>3+</sup> distribution. The molar volume model with unary and binary model parameters can be used to predict the molar volume of the molten oxide of the Li<sub>2</sub>O-Na<sub>2</sub>O-K<sub>2</sub>O-MgO-CaO-MnO-PbO-FeO-Fe<sub>2</sub>O<sub>3</sub>-Al<sub>2</sub>O<sub>3</sub>-SiO<sub>2</sub> system in the entire range of compositions, temperatures, and oxygen partial pressures from Fe saturation to 1 atm pressure.

DOI: 10.1007/s11663-015-0549-x

© The Minerals, Metals & Materials Society and ASM International 2015

## I. INTRODUCTION

MANY slag systems in the steelmaking process and non-ferrous metallurgical process contain significant amounts of iron oxide. For example, the CaO-FeO-Fe<sub>2</sub>O<sub>3</sub>-SiO<sub>2</sub> slag is the main slag system of both the basic oxygen furnace (steelmaking process) and converter process of non-ferrous metals such as Cu and Zn. In addition, the slags for ferro-alloy production and electric arc furnace slags for steel production contain a large amount of iron oxide. Molar volume or density is one of the most fundamental physical properties of liquid slags and is required for the design of industrial processes. However, the molar volume of Fe oxide-containing slag is complex because of the redox reaction in slag producing both FeO and Fe<sub>2</sub>O<sub>3</sub> in liquid state. The amount of FeO and Fe<sub>2</sub>O<sub>3</sub> changes with slag composition, temperature, and oxygen partial pressure.

Critical evaluation of all experimental molar volume data in the Li<sub>2</sub>O-Na<sub>2</sub>O-K<sub>2</sub>O-MgO-CaO-MnO-PbO-Al<sub>2</sub>O<sub>3</sub>-SiO<sub>2</sub> system, the modeling of molar volume of unary and binary melts, and demonstration of predictive ability of the present structural molar volume model in ternary and multicomponent melts were already presented in the Parts I and II of this series of studies.<sup>[1,2]</sup>

The purpose of the present study is to critical review of the experimental molar volume data of the FeO-Fe<sub>2</sub>O<sub>3</sub>-Na<sub>2</sub>O-K<sub>2</sub>O-MgO-CaO-MnO-Al<sub>2</sub>O<sub>3</sub>-SiO<sub>2</sub> system and modeling based on a structural molar volume

model. The molar volume parameters of pure FeO and Fe<sub>2</sub>O<sub>3</sub> and hypothetical binary FeO-SiO<sub>2</sub> and Fe<sub>2</sub>O<sub>3</sub>-SiO<sub>2</sub> melts were optimized in the present study based on the most reliable experimental data. Then the molar volumes of all ternary and multicomponent melts under any oxygen partial pressure can be accurately predicted from the present structure molar volume model.

## II. STRUCTURAL MOLAR VOLUME MODEL

A structural molar volume model for binary systems was presented in Part I of this study and its expansion to ternary and multicomponent systems was explained in Part II. A short review of the model is given below.

The total number of oxygen ( $n_t$ ) in one mole of a M<sub>2</sub>O-...-MO-...-M<sub>2</sub>O<sub>3</sub>-...-SiO<sub>2</sub> melt (where M is any metallic cation such as Na, Ca, Mg, Fe(II), Al, Fe(III), etc.) is

$$n_t = X_{M_2O} + \dots + X_{MO} + \dots + 3X_{M_2O_3} + \dots + 2X_{SiO_2}, \quad [1]$$

where  $X$  is the mole fraction of each respective oxide in the melt. Then the number of bridged oxygen ( $n_{O^\circ}$ ) in one mole of solution can be calculated by multiplying the mole fraction of Si-Si pairs ( $X_{Si-Si}$ ) in the solution, calculated by the Modified Quasichemical Model (MQM)<sup>[3]</sup> with an optimized thermodynamic database (FactSage FToxid database<sup>[4]</sup>):  $n_{O^\circ} = X_{Si-Si}n_t$ . Strictly speaking, Al<sub>2</sub>O<sub>3</sub> and Fe<sub>2</sub>O<sub>3</sub> behave as amphoteric components in molten slags. However, for the sake of simplicity, Al<sub>2</sub>O<sub>3</sub> and Fe<sub>2</sub>O<sub>3</sub> were treated in the present model as network modifiers like Na<sub>2</sub>O, CaO, MgO, FeO, etc. The amount of different silicate tetrahedral Q<sup>n</sup> species in one mole of given melt can be calculated based on the random distribution of bridged and broken oxygen around each Si atom in silicate melt. In addition, the amount of free oxygen bond units,  $n_{M-M}$  per mole of melt, can be calculated to be  $n_{M-M} = X_{M-M}n_t$ , where M = all cationic species like

ERIC THIBODEAU, Graduate Student, and IN-HO JUNG, Associate Professor, are with the Department of Mining and Materials Engineering, McGill University, 3610 University Street, Montreal, QC H3A 0C5, Canada. Contact e-mail: in-ho.jung@mcgill.ca AIMEN E. GHERIBI, Research Associate, is with the Centre de Recherche en Calcul Thermochimique, Département de Génie Chimique, Ecole Polytechnique de Montreal, C.P. 6079, Succ. Centre-ville, Montreal, QC H3C3A7, Canada.

Manuscript submitted November 27, 2014.

Article published online December 30, 2015.

**Table I. Optimized Molar Volume Model Parameters for Unary and Binary Fe Oxide Silicate Systems**

Oxides	Q <sup>3</sup>		Q <sup>2</sup>		Q <sup>1</sup>		Q <sup>0</sup>		Pure Oxide		Linear <sup>#1</sup>	
	<i>a</i>	<i>b</i> × 10 <sup>3</sup>	<i>a</i>	<i>b</i> × 10 <sup>3</sup>	<i>a</i>	<i>b</i> × 10 <sup>3</sup>	<i>a</i>	<i>b</i> × 10 <sup>3</sup>	<i>a</i>	<i>b</i> × 10 <sup>3</sup>	<i>a</i>	<i>b</i> × 10 <sup>3</sup>
FeO	27.00	2.00	37.00	3.00	38.00	4.00	41.00	7.00	13.46	1.25	8.76	2.92
Fe <sub>2</sub> O <sub>3</sub>	45.00	0.00	45.00	0.00	70.00	0.00	70.00	0.00	10.05	1.38	26.92	9.09
SiO <sub>2</sub> (Q <sup>4</sup> )	—	—	—	—	—	—	—	—	27.3	0.00	26.9	0.00

*a* is in cm<sup>3</sup>/mole and *b* is in cm<sup>3</sup>/mole-K.

#1: The model parameters for a linear model obtained from the work of Lange and Carmichael.<sup>[5]</sup>

Na, Ca, Mg, Fe(II), Al, Fe(III), except Si in given melt.

The molar volume of binary silicate MO-SiO<sub>2</sub> melts is calculated from the molar volume of MO and SiO<sub>2</sub> and Q<sup>*n*</sup> species using the following formula:

$$V_m = n_{Q^n}(a_{SiO_2} + b_{SiO_2}T) + \sum_{n=0}^3 n_{Q^n}(a_n + b_nT) \quad [2]$$

$$+ n_t x_{M-M}(a_{M-M} + b_{M-M}T),$$

where molar volume of each unit in the model is expressed as a function of temperature, *a* + *bT*. The unary molar volume parameters and binary Q<sup>*n*</sup> species parameters were determined based on unary and binary molar volume data.

In order to predict the molar volume of ternary and multicomponent slags, the quantity of each Q<sup>*n*</sup> species for a given melt can be calculated from pair (bond) fraction information using the MQM model<sup>[3]</sup> with FactSage FTOxid database.<sup>[4]</sup> Then, the molar volume of the melt can be calculated using the following formula based on a linear extrapolation of the unary and binary parameters weighted by the quantity of each M-Si pairs:

$$V_m = n_{Q^n}(a_{SiO_2} + b_{SiO_2}T) + \sum_{n=0}^3 n_{Q^n} \frac{\sum_i x_{Si-i}(a_{ni} + b_{ni}T)}{\sum_i x_{Si-i}}$$

$$+ n_t \sum_i \sum_j x_{i-j}(a_{i-j} + b_{i-j}T), \quad [3]$$

where *n*<sub>Q<sup>*n*</sup></sub> and *n*<sub>*t*</sub> are the number of moles of Q<sup>*n*</sup> species and total oxygen in one mole of liquid. *x*<sub>Si-*i*</sub> and *x*<sub>*i*-*i*</sub> are bond fractions of broken oxygen (*Si-*i* pairs) and free oxygen (*i-*j* pairs where *i* and *j* are cations other than Si) in one mole of liquid. The molar volume parameters of pure SiO<sub>2</sub> (*a*<sub>SiO<sub>2</sub></sub> + *b*<sub>SiO<sub>2</sub></sub>*T*), Q<sup>*n*</sup> (*a*<sub>*nM*</sub> + *b*<sub>*nM*</sub>*T*), where *n* = 0 to 3, and MO (*a*<sub>M-M</sub> + *b*<sub>M-M</sub>*T*) are obtained by the reproduction of the molar volume change in the binary a MO-SiO<sub>2</sub> melt. The last term in Eq. [3] incorporates the effect of free oxygen species. The molar volume of M<sub>*i*</sub>-M<sub>*j*</sub> (*a*<sub>*i-j*</sub> + *b*<sub>*i-j*</sub>*T*) is the average of the molar volume of M<sub>*i*</sub>-M<sub>*i*</sub> (*a*<sub>*i-i*</sub> + *b*<sub>*i-i*</sub>*T*) and M<sub>*j*</sub>-M<sub>*j*</sub> (*a*<sub>*j-j*</sub> + *b*<sub>*j-j*</sub>*T*). In the case of Na<sub>2</sub>O containing system, Na<sub>2</sub> is considered as network modified cation species. That is, Na<sub>2</sub> is M in Eqs. [2] and [3]. The same is applied for other alkali oxides. It should be noted that there is no ternary or higher order correction term in Eq. [3]. Once unary and binary Q<sup>*n*</sup> species parameters are determined, accurate prediction of molar volume of ternary and multicomponent systems can be done by the model.**

The last term in Eq. [3] incorporates the effect of free oxygen species (*e.g.*, Na-Na, Ca-Ca, Na-Ca, *etc.*). That is, if there is no SiO<sub>2</sub> in the melt, the molar volume of the slag can be calculated only from the last term. Therefore, the molar volume of binary molten slag with no SiO<sub>2</sub> changes linearly in the present model. For example, the molar volume of the ternary CaO-FeO-Fe<sub>2</sub>O<sub>3</sub> slag varies linearly, from the present model, dependent on the amount of each component in slag. This will be discussed later.

The molar volume of the Na<sub>2</sub>O-K<sub>2</sub>O-MgO-CaO-MnO-Al<sub>2</sub>O<sub>3</sub>-SiO<sub>2</sub> slag was already fully modeled in the Parts I<sup>[1]</sup> and II.<sup>[2]</sup> The model parameters can be found in Part I.<sup>[1]</sup> So, the addition of FeO and Fe<sub>2</sub>O<sub>3</sub> to this multicomponent slag only requires the molar volume model parameters for unary FeO and Fe<sub>2</sub>O<sub>3</sub> and binary FeO-SiO<sub>2</sub> and Fe<sub>2</sub>O<sub>3</sub>-SiO<sub>2</sub>. The model parameters are listed in Table I. The details of modeling process are discussed below.

### III. CRITICAL EVALUATION AND OPTIMIZATION OF MOLAR VOLUME

In order to develop an accurate molar volume model containing iron oxide, an accurate thermodynamic database to calculate the amount of Fe<sup>2+</sup> and Fe<sup>3+</sup> in liquid slag under any partial pressure of oxygen is required. In FactSage FTOxid database,<sup>[4]</sup> critically evaluated and optimized model parameters for liquid slag with FeO-Fe<sub>2</sub>O<sub>3</sub>-SiO<sub>2</sub>-CaO-MgO-MnO-Al<sub>2</sub>O<sub>3</sub>-*etc.*, components are stored. During the optimization of the thermodynamic model, the phase equilibria between slag and gas to quantify the variation of Fe<sup>2+</sup> and Fe<sup>3+</sup> as a function of oxygen partial pressure, composition, and temperature; the phase diagram data of Fe saturation, air, and various oxygen partial pressures; the activity data for liquid slag, *etc.*, are all taken into account. Some of the published results for the optimization for FeO-Fe<sub>2</sub>O<sub>3</sub>,<sup>[6]</sup> FeO-Fe<sub>2</sub>O<sub>3</sub>-SiO<sub>2</sub>,<sup>[7]</sup> FeO-Fe<sub>2</sub>O<sub>3</sub>-MgO,<sup>[8]</sup> FeO-Fe<sub>2</sub>O<sub>3</sub>-CaO,<sup>[9]</sup> FeO-Fe<sub>2</sub>O<sub>3</sub>-Al<sub>2</sub>O<sub>3</sub>,<sup>[9]</sup> FeO-Fe<sub>2</sub>O<sub>3</sub>-CaO-SiO<sub>2</sub>,<sup>[9]</sup> FeO-Fe<sub>2</sub>O<sub>3</sub>-MgO-SiO<sub>2</sub>,<sup>[10]</sup> FeO-Fe<sub>2</sub>O<sub>3</sub>-MnO-Mn<sub>2</sub>O<sub>3</sub>-SiO<sub>2</sub><sup>[11]</sup> systems are available in the literature.

The bond fractions of liquid slags containing iron oxide were calculated from the MQM<sup>[3]</sup> with optimized thermodynamic model parameters from FactSage FTOxid database.<sup>[4]</sup> The structural units for the molar volume are then calculated from the bond fraction data.

Table II. Summary of Experimental Data of Iron Oxide-Bearing Melts

System	Reference (Year: Authors)	Method <sup>a</sup>	Data Presentation	Condition	
FeO <sub>x</sub>	1961: Henderson <i>et al.</i> <sup>[12]</sup>	MBP	table	Fe Sat. (Ar)	
	1963: Adachi <i>et al.</i> <sup>[13]</sup>	DBA, SBA	graph	Fe Sat. (Ar)	
	1964: Henderson <sup>[14]</sup>	MBP	table	Fe Sat. (Ar)	
	1965: Ward and Sachdev <sup>[15]</sup>	MBP	table	Fe Sat. (N <sub>2</sub> )	
	1967: Gaskell and Ward <sup>[16]</sup>	MBP	table	Fe Sat. (Ar, He, N <sub>2</sub> )	
	1968: Mori and Suzuki <sup>[17]</sup>	DBA	graph	variable CO/CO <sub>2</sub> (not specified)	
	1970: Sokolov <i>et al.</i> <sup>[18]</sup>	MBP	table	Fe Sat. (He)	
	1974: Lee and Gaskell <sup>[19]</sup>	MBP	table	variable P <sub>O2</sub> (not specified)	
	1974: Ogino <i>et al.</i> <sup>[20]</sup>	DBA	graph	Fe Sat. (N <sub>2</sub> , Ar)	
	1976: Kawai <i>et al.</i> <sup>[21]</sup>	MBP	equation	Fe Sat. (Ar)	
	1978: Shiraishi <i>et al.</i> <sup>[22]</sup>	SBA	table	Fe Sat. (Ar)	
	1988: Hara <i>et al.</i> <sup>[23]</sup>	DBA	table	air, CO <sub>2</sub> /H <sub>2</sub> , CO <sub>2</sub>	
	CaO-FeO <sub>x</sub>	1964: Henderson <sup>[14]</sup>	MBP	table	Fe Sat. (Ar)
		1974: Lee and Gaskell <sup>[19]</sup>	MBP	table	variable P <sub>O2</sub> (not specified)
1974: Ogino <i>et al.</i> <sup>[20]</sup>		DBA	graph	Fe Sat. (N <sub>2</sub> , Ar)	
1975: Abrodimov <sup>[24]</sup>		MBP	graph	(assumed Fe Sat. and air)	
1976: Kawai <i>et al.</i> <sup>[21]</sup>		MBP	equation	Fe Sat. (Ar)	
1983: Sumita <i>et al.</i> <sup>[25]</sup>		DBA	graph	air	
Na <sub>2</sub> O-FeO <sub>x</sub>	1988: Hara <i>et al.</i> <sup>[23]</sup>	DBA	table	air, CO <sub>2</sub> /H <sub>2</sub> , CO <sub>2</sub>	
	2006: Vadasz <i>et al.</i> <sup>[43]</sup>	MBP	table	air	
FeO <sub>x</sub> -SiO <sub>2</sub>	1983: Sumita <i>et al.</i> <sup>[25]</sup>	DBA	graph	air	
	1961: Henderson <i>et al.</i> <sup>[12]</sup>	MBP	table	Fe Sat. (Ar)	
	1962: Adachi and Ogino <sup>[26]</sup>	MBP	table	Fe Sat. (N <sub>2</sub> )	
	1963: Adachi <i>et al.</i> <sup>[13]</sup>	DBA	graph	Fe Sat. (Ar)	
	1964: Henderson <sup>[14]</sup>	MBP	table	Fe Sat. (Ar)	
	1965: Ward and Sachdev <sup>[15]</sup>	MBP	table	Fe Sat. (N <sub>2</sub> )	
	1967: Gaskell and Ward <sup>[16]</sup>	MBP	table	Fe Sat. (Ar, He, N <sub>2</sub> )	
	1969: Gaskell <i>et al.</i> <sup>[27]</sup>	MBP	table	Fe Sat. (Ar)	
	1970: Sokolov <i>et al.</i> <sup>[18]</sup>	MBP	table	Fe Sat. (He)	
	1972: Holeczy <i>et al.</i> <sup>[28]</sup>	MBP	table	(assume Fe Sat.)	
	1974: Lee and Gaskell <sup>[19]</sup>	MBP	table	variable P <sub>O2</sub> (not specified)	
	1974: Ogino <i>et al.</i> <sup>[20]</sup>	DBA	graph	Fe Sat. (N <sub>2</sub> , Ar)	
	1976: Kawai <i>et al.</i> <sup>[21]</sup>	MBP	equation	Fe Sat. (Ar)	
	1978: Shiraishi <i>et al.</i> <sup>[22]</sup>	DBA	table	Fe Sat. (Ar)	
	1982: Mo <i>et al.</i> <sup>[29]</sup>	DBA	equation	Fe Sat. (N <sub>2</sub> , Ar)	
	1997: Courtial <i>et al.</i> <sup>[30]</sup>	DBA	table	Air	
	Na <sub>2</sub> O-FeO <sub>x</sub> -SiO <sub>2</sub>	2013: Thomas	DBA	table	1 pct CO—99 pct Ar
		1982: Mo <i>et al.</i> <sup>[29]</sup>	DBA	equation	air
		1987: Lange and Carmichael <sup>[31]</sup>	DBA	table	air
		1988: Dingwell <i>et al.</i> <sup>[32]</sup>	DBA	table	air
2006: Liu and Lange <sup>[33]</sup>		DBA	table	air	
K <sub>2</sub> O-FeO <sub>x</sub> -SiO <sub>2</sub>	2013: Guo <sup>[34]</sup>	DBA	table	1 pct CO—99 pct Ar	
	2006: Liu and Lange <sup>[33]</sup>	DBA	table	air	
CaO-FeO <sub>x</sub> -Al <sub>2</sub> O <sub>3</sub>	1977: Zielinski and Sikora <sup>[35]</sup>	MBP	table	air	
	2000: Vadasz <sup>[36]</sup>	MBP	table	air	
FeO <sub>x</sub> -Al <sub>2</sub> O <sub>3</sub> -SiO <sub>2</sub>	1975: Abrodimov <sup>[24]</sup>	MBP	graph	(assumed Fe Sat. and air)	
MgO-FeO <sub>x</sub> -SiO <sub>2</sub>	1968: Bryantsev <sup>[37]</sup>	MBP	table	Fe Sat. (Ar)	
	1960: Adachi <i>et al.</i> <sup>[38]</sup>	MBP	graph	Fe Sat. (N <sub>2</sub> )	
CaO-FeO <sub>x</sub> -SiO <sub>2</sub>	1962: Adachi and Ogino <sup>[26]</sup>	MBP	table	Fe Sat. (N <sub>2</sub> )	
	1962: Wu <i>et al.</i> <sup>[39]</sup>	MBP	table	Fe Sat. (Ar)	
	1964: Henderson <sup>[14]</sup>	MBP	table	Fe Sat. (Ar)	
	1969: Gaskell <i>et al.</i> <sup>[27]</sup>	MBP	table	Fe Sat. (Ar)	
	1970: Sokolov <i>et al.</i> <sup>[18]</sup>	MBP	table	Fe Sat. (He)	
	1974: Lee and Gaskell <sup>[19]</sup>	MBP	table	variable P <sub>O2</sub> (not specified)	
	1974: Ogino <i>et al.</i> <sup>[20]</sup>	DBA	graph	Fe Sat. (N <sub>2</sub> , Ar)	
	1975: Abrodimov <i>et al.</i> <sup>[24]</sup>	MBP	graph	(assumed Fe Sat. and air)	
	1976: Kawai <i>et al.</i> <sup>[21]</sup>	MBP	equation	Fe Sat. (Ar)	
	1982: Mo <i>et al.</i> <sup>[29]</sup>	DBA	equation	air	
	1985: Licko <i>et al.</i> <sup>[40]</sup>	SBA	equation	air	
	1988: Dingwell and Brearly <sup>[41]</sup>	DBA	table	air	
	1988: Hara <i>et al.</i> <sup>[23]</sup>	DBA	table	air, CO <sub>2</sub> /H <sub>2</sub> , CO <sub>2</sub>	
	2000: Vadasz <i>et al.</i> <sup>[36]</sup>	MBP	table	air	
2013: Guo <sup>[34]</sup>	DBA	table	1 pct CO—99 pct Ar		

Table II. continued

System	Reference (Year: Authors)	Method <sup>a</sup>	Data Presentation	Condition
CaO-MgO-FeO <sub>x</sub>	2006: Vadasz <i>et al.</i> <sup>[43]</sup>	MBP	table	air
MnO-FeO <sub>x</sub> -SiO <sub>2</sub>	1969: Gaskell <i>et al.</i> <sup>[27]</sup>	MBP	table	Fe Sat. (Ar)
	1970: Sokolov <i>et al.</i> <sup>[18]</sup>	MBP	table	Fe Sat. (He)
	1974: Ogino <i>et al.</i> <sup>[20]</sup>	DBA	graph	Fe Sat. (N <sub>2</sub> , Ar)
Higher order system	1968: Bryantsev <sup>[37]</sup>	MBP	table	Fe Sat. (Ar)
	1970: Sokolov <i>et al.</i> <sup>[18]</sup>	MBP	table	Fe Sat. (He)
	1979: Nelson and Carmichael <sup>[42]</sup>	DBA	equation	(assume Fe Sat.)
	1982: Mo <i>et al.</i> <sup>[29]</sup>	DBA	equation	air
	1997: Courtial <i>et al.</i> <sup>[30]</sup>	DBA	table	air
	2013: Guo <sup>[34]</sup>	DBA	table	1 pct CO—99 pct Ar

<sup>a</sup>Method: DBA = Double Bob Archimedean; SDA = Single Bob Archimedean; MBP = Maximum Bubble Pressure.

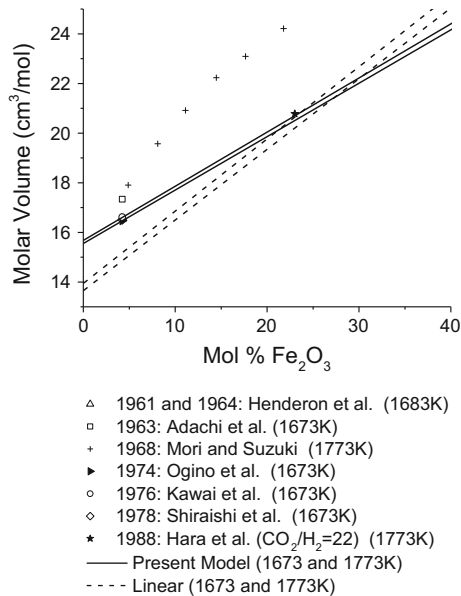


Fig. 1—The molar volume of the binary FeO-Fe<sub>2</sub>O<sub>3</sub> system at 1673 K and 1773 K (1400 °C and 1500 °C).<sup>[12–14,17,20–25]</sup> The data point at the lowest Fe<sub>2</sub>O<sub>3</sub> content, iron saturation, represents multiple data from various research groups. Experimental condition for each study can be found in Table II.

Structural changes are automatically taken into account in the molar volume calculations as described in Eqs. [2] and [3]. All the volume parameters used in this work are listed in Part I<sup>[1]</sup> of this study and new parameters related to FeO and Fe<sub>2</sub>O<sub>3</sub> are listed in Table I. The summary of experimental data for iron oxide-containing slags is presented in Table II. The present modeling results are also compared with the results of the linear model developed by Lange and Carmichael.<sup>[5]</sup>

### A. FeO-Fe<sub>2</sub>O<sub>3</sub> System

The density of the iron oxide system has been primarily studied in contact with solid iron under an inert atmosphere. Only Mori and Suzuki<sup>[17]</sup> and Hara *et al.*<sup>[23]</sup> examined the melts under controlled oxygen partial pressures.

The density measurements of iron oxide melts in contact with iron (iron saturation) are relatively

scattered. It was noted in earlier works that the density of iron oxide melts (and other iron oxide-rich melts) could be varied depending on the inert gas used. Ward and Sachdev<sup>[15]</sup> demonstrated that they could obtain very different results depending on whether they used Ar or N<sub>2</sub> atmosphere while using the MBP method. This effect was later attributed to the precipitation of iron from the melt due to the differences in thermal conductivities of the inert gases. The deviation between the results obtained using different inert gases could be eliminated with better temperature control. Gaskell and Ward<sup>[16]</sup> performed improved measurements using Ar, N<sub>2</sub>, and He gas and obtained virtually the same results. Therefore, it should be noted that in some of the earlier works there is the possibility of iron precipitation which significantly increases the apparent density of the melt (lowers the molar volume) depending on the inert gas used. Early results using Ar gas are comparable with the more recent/accurate results.

The optimized molar volume of the FeO-Fe<sub>2</sub>O<sub>3</sub> system is shown in Figure 1 along with experimental data. Both the linear model and the present model assume a linear extrapolation across the system. A subset of the data in iron saturation has been shown, as there are too many data points to illustrate while maintaining clarity. In iron saturation, the most accurate results are believed to be those of Ogino *et al.*<sup>[20]</sup> using a DBA technique (tabulated) in both Ar and N<sub>2</sub> atmospheres. Density values of between 4.58 and 4.59 g/cm<sup>3</sup> at 1673 K (1400 °C) were obtained. These values are consistent with the more recent values by Shiraishi *et al.*<sup>[22]</sup> who used a SBA technique (tabulated) with correction of surface tension contributions.

Mori and Suzuki<sup>[17]</sup> varied oxygen partial pressure by controlling the CO/CO<sub>2</sub> ratio and used a DBA method. They reported their density measurements graphically, and only published their Fe<sup>3+</sup>/Fe ratios without oxygen partial pressure information. It was not possible to calculate the ferric to ferrous ratios using FactSage and therefore the raw data were used as reported. Hara *et al.*<sup>[23]</sup> measured a single composition with a CO<sub>2</sub>/H<sub>2</sub> ratio of 22, using a DBA method. The present model and the linear model of Lange and Carmichael<sup>[5]</sup> are illustrated at two temperatures [1673 K and 1773 K (1400 °C and 1500 °C)]. The results of Lange and Carmichael may not reproduce the data exactly because all the

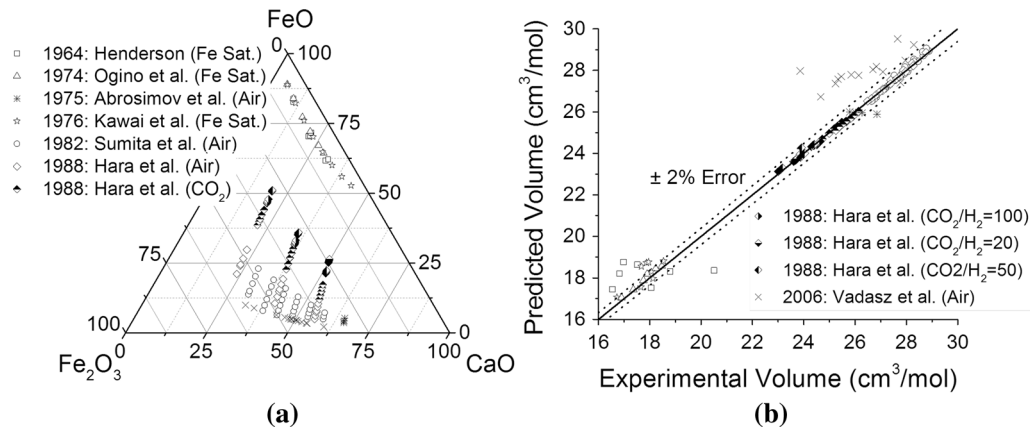


Fig. 2—The ternary CaO-FeO-Fe<sub>2</sub>O<sub>3</sub> system: (a) compositions (mol pct) examined and (b) model accuracy.<sup>[14,20,21,23–25,43]</sup>

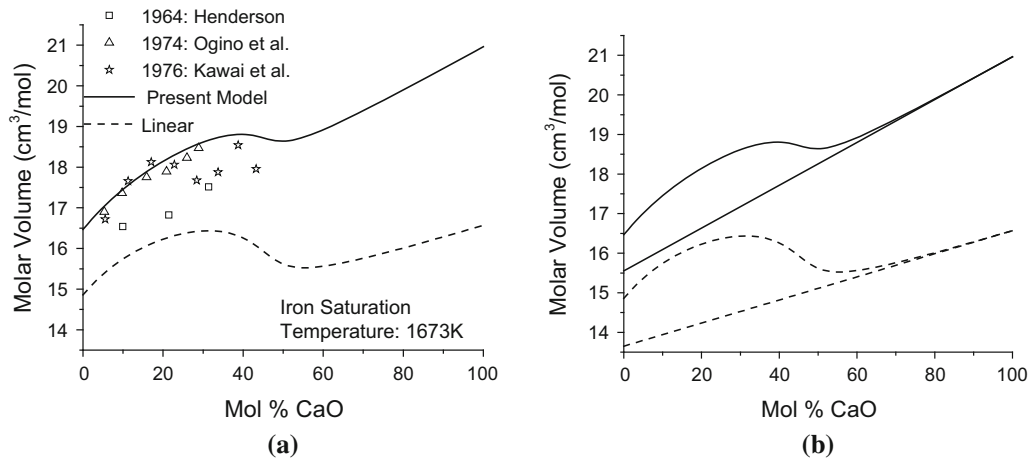


Fig. 3—The (a) ternary CaO-FeO-Fe<sub>2</sub>O<sub>3</sub> system in iron saturation at 1673 K (1400 °C),<sup>[14,20,21]</sup> and (b) calculated molar volumes of the theoretical binary CaO-FeO system (straight lines) in comparison to those of real CaO-FeO<sub>x</sub> system under iron saturation (curved lines) at 1673 K (1400 °C).

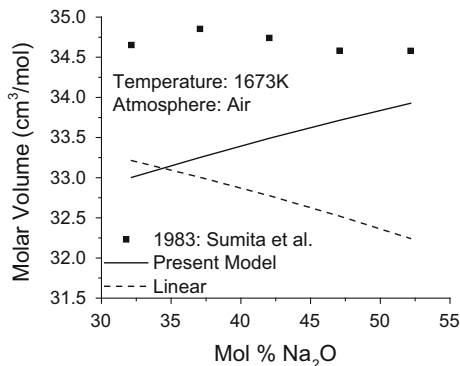


Fig. 4—The molar volume of ternary Na<sub>2</sub>O-FeO-Fe<sub>2</sub>O<sub>3</sub> system in air at 1673 K (1400 °C).<sup>[25]</sup>

experimental data used in this work were analyzed using FactSage. The calculate the ferric to ferrous ratios do not coincide exactly with the values used by Lange and Carmichael for the calibration of their model parameters. In addition, the model of Lange and Carmichael was

calibrated primarily using the experimental data of melts studied in air and in relatively silica-rich compositions.

The experimental data of Mori and Suzuki are inconsistent with the more recent data of Hara *et al.* The results published by Mori and Suzuki suggest a non-linear variation in molar volume between FeO and Fe<sub>2</sub>O<sub>3</sub>. It is unknown why their results differ from Hara *et al.* The transcription of their results and the uncertainty of the Fe<sup>3+</sup>/Fe content does not explain the deviation. The present model is in good agreement with the most recent experimental results with iron saturation using various techniques. The molar volumes of FeO and Fe<sub>2</sub>O<sub>3</sub> were numerically optimized by performing a multi-linear regression on the data of Hara *et al.*,<sup>[23]</sup> Ogino *et al.*,<sup>[23]</sup> and Sumita *et al.*<sup>[25]</sup> with the experimental data of the CaO-FeO-Fe<sub>2</sub>O<sub>3</sub> system.

## B. Ternary Systems

### 1. CaO-FeO-Fe<sub>2</sub>O<sub>3</sub> system

This silica-free ternary system in iron saturation was examined by Henderson<sup>[14]</sup> (MBP), Ogino *et al.*<sup>[20]</sup> (DBA), and Kawai *et al.*<sup>[21]</sup> (MBP). Abrosimov

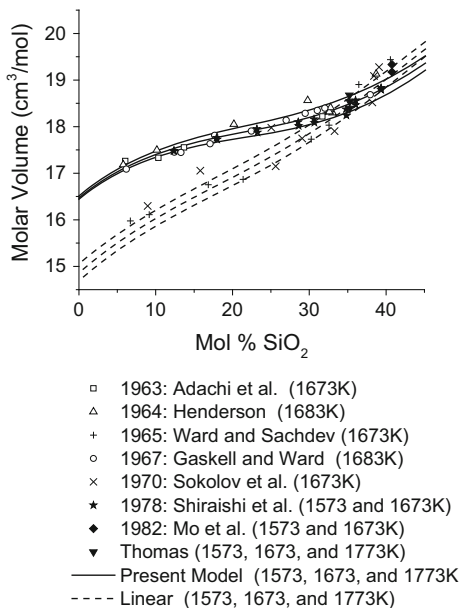


Fig. 5—The ternary FeO-Fe<sub>2</sub>O<sub>3</sub>-SiO<sub>2</sub> system in iron saturation at 1573 K, 1673 K, and 1773 K (1300 °C, 1400 °C, and 1500 °C).<sup>[13-16,18,22,29,44]</sup> Molar volumes increase with temperature for both the present model and the linear model and this is also true for the data presented for authors at multiple temperatures.

*et al.*<sup>[24]</sup> (MBP), Sumita *et al.*<sup>[25]</sup> (DBA), Hara *et al.*<sup>[23]</sup> (DBA), and Vadasz *et al.*<sup>[43]</sup> (MBP) all examined this system in air. Hara *et al.*<sup>[23]</sup> (DBA) and Lee and Gaskell<sup>[19]</sup> (MBP) varied the oxygen partial pressure. Unfortunately, Lee and Gaskell did not provide the partial pressures used; therefore, their results have been omitted from this comparison.

The compositions studied by each research group along with the experimental condition and the accuracy of the present model are shown Figure 2. This system is well reproduced with a linear model, as demonstrated in the work of Hara *et al.*<sup>[23]</sup> at various oxygen partial pressures. The model parameters used for CaO, FeO, and Fe<sub>2</sub>O<sub>3</sub> in this work can reproduce all the most accurate experimental data. The work by Ogino *et al.*, Sumita *et al.*, and Hara *et al.* were all performed using accurate DBA techniques and are reproduced well within 2 pct error. The data obtained from MBP measurements are less well reproduced. In iron oxide-bearing systems, the MBP method appears to provide very poor and inconsistent results compared to the DBA method.

The molar volume of this system in iron saturation is shown in Figure 3(a). Although it is with iron saturation, there are a certain amount of Fe<sub>2</sub>O<sub>3</sub> in the melt. A significant curvature is noted in the high-FeO<sub>3</sub> region. This is due to the local maximum of the Fe<sup>3+</sup>/Fe<sup>2+</sup> ratio at approximately 25 mol pct CaO in iron saturation. For illustrative purposes, the molar volume assuming no Fe<sub>2</sub>O<sub>3</sub> (that is, FeO-CaO) for both the present model and the linear model is shown in Figure 3(b).

## 2. Na<sub>2</sub>O-FeO-Fe<sub>2</sub>O<sub>3</sub> system

The Na<sub>2</sub>O-FeO-Fe<sub>2</sub>O<sub>3</sub> system was studied in air by Sumita *et al.*<sup>[25]</sup> using the DBA (graphical) method. The

results were published as the Fe<sub>2</sub>O<sub>3</sub>-Na<sub>2</sub>O system with the addition of Na<sub>2</sub>O in air. The measurements at 1673 K (1400 °C) are shown in Figure 4. Both the present model and the linear model fail to reproduce the experimental data. Both models predict lower molar volumes. There are several potential explanations for this failing. It is possible that the calculations by FactSage are incorrect in estimating the Fe<sup>3+</sup> content in sodium-bearing melts; the database of the Na<sub>2</sub>O-FeO-Fe<sub>2</sub>O<sub>3</sub> system is still under development. Another possibility is that there is an interaction between ferric iron oxide and sodium oxide which results in the formation of an associate with a larger molar volume. The linear model and the present model provide opposite trends; the linear model of Lange and Carmichael assumes a smaller volume of Na<sub>2</sub>O and a larger volume of iron oxide in air than the present model.

## 3. FeO-Fe<sub>2</sub>O<sub>3</sub>-SiO<sub>2</sub> system

This ternary system was primarily studied in contact with solid iron (iron saturation) or in such highly reducing conditions that they could be approximated as being in iron saturation. Only a single measurements has been performed in air, by Courtial *et al.*<sup>[30]</sup> using the DBA technique. Due to the quantity of the experimental data in iron saturation, only the most systematic or the most accurate data are shown in Figure 5 to maintain clarity.

All the results obtained from DBA measurements (Adachi *et al.*<sup>[13]</sup> (1963), Ogino *et al.*<sup>[20]</sup> Shiraishi *et al.*<sup>[22]</sup> Mo *et al.*<sup>[29]</sup> and Thomas<sup>[44]</sup>) are self-consistent. These data were used for the optimization of the FeO-SiO<sub>2</sub> system with more emphasis on the data of Shiraishi *et al.* The study by Shiraishi *et al.* spanned the widest composition range, provided results at multiple temperatures, used an accurate DBA technique, and tabulated their results. The results obtained from MBP methods are less consistent. For example, the results of Henderson<sup>[14]</sup> and Gaskell and Ward<sup>[16]</sup> follow the same trend as those of Shiraishi *et al.* but with more scatter. The results of Sokolov *et al.*<sup>[18]</sup> and Ward and Sachdev<sup>[15]</sup> are both believed to have precipitated iron, increasing the density and lowering the molar volume. The linear model of Lange and Carmichael does not reproduce the most accurate data in the iron oxide-rich region. Any curvature in the model of Lange and Carmichael is due to the variation of ferrous to ferric ratio with SiO<sub>2</sub> content in the system. The FeO-SiO<sub>2</sub> system with Fe saturation was optimized by fitting the data of Shiraishi *et al.* and ensuring a smooth trend from the SiO<sub>2</sub>-rich region.

The hypothetical molar volume of the FeO-SiO<sub>2</sub> melt is calculated in Figure 6. The result of the present model is very similar to the results from the linear model by Lange and Carmichael above 33 mol pct SiO<sub>2</sub>.

The Fe<sub>2</sub>O<sub>3</sub>-SiO<sub>2</sub> system could not be optimized in a similar manner as the FeO-SiO<sub>2</sub> system due to lack of experimental data. Therefore, it was optimized by assuming all the temperature dependence terms were equal to zero (as was done in the Al<sub>2</sub>O<sub>3</sub>-SiO<sub>2</sub> system) and optimized based on experimental data in higher order systems using the DBA method. The calculated

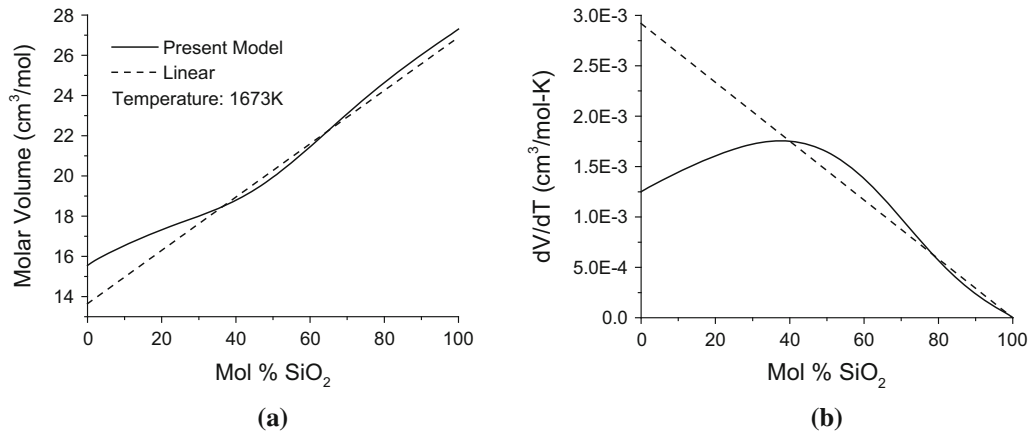


Fig. 6—Molar volume of the hypothetical binary FeO-SiO<sub>2</sub> system at (a) 1673 K (1400 °C) and (b) temperature dependence.

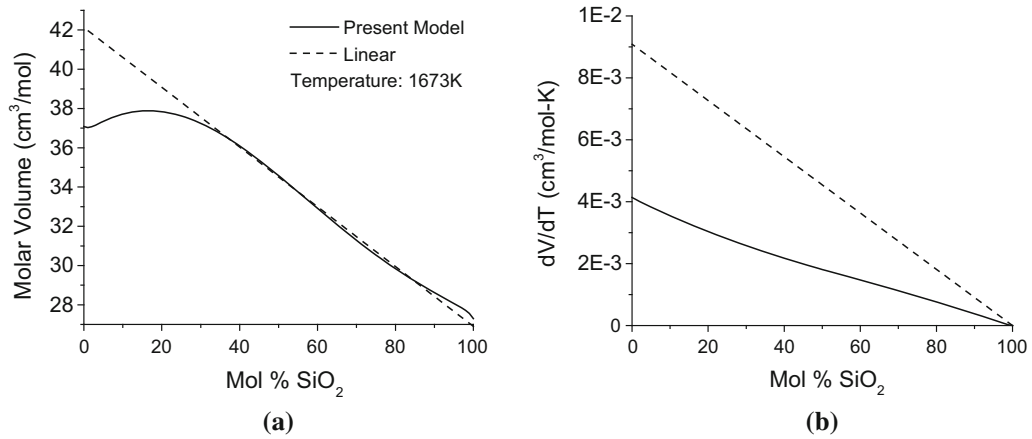


Fig. 7—The molar volume of the hypothetical binary Fe<sub>2</sub>O<sub>3</sub>-SiO<sub>2</sub> system at (a) 1673 K (1400 °C) and (b) temperature dependence.

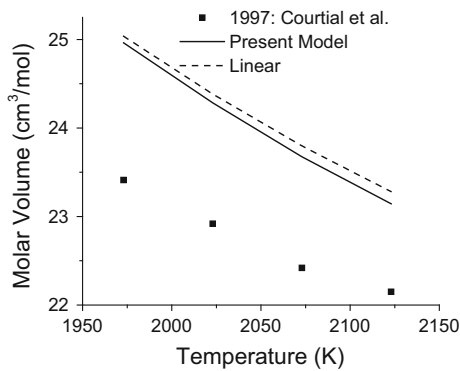


Fig. 8—The molar volume of the ternary FeO-Fe<sub>2</sub>O<sub>3</sub>-SiO<sub>2</sub> system in air at ~37 mol pct SiO<sub>2</sub> as a function of temperature.<sup>[30]</sup>

molar volume of a hypothetical Fe<sub>2</sub>O<sub>3</sub>-SiO<sub>2</sub> system is shown in Figure 7. The variation of molar volume at 1673 K (1400 °C) is consistent with the results obtained by the linear model Lange and Carmichael in the high SiO<sub>2</sub> region but deviates at low SiO<sub>2</sub> region due to the restriction imposed by the molar volume of pure Fe<sub>2</sub>O<sub>3</sub>. As the binary parameters are temperature independent,

the temperature dependence of molar volume in Figure 7(b) results from by those of pure Fe<sub>2</sub>O<sub>3</sub> and SiO<sub>2</sub>.

In air, only a single composition of the FeO-Fe<sub>2</sub>O<sub>3</sub>-SiO<sub>2</sub> system (at ~37 mol pct SiO<sub>2</sub>) was examined by Courtial *et al.*<sup>[30]</sup> (DBA) and their results are shown in Figure 8. The experimental molar volume of FeO-Fe<sub>2</sub>O<sub>3</sub>-37 mol pct SiO<sub>2</sub> decreased with temperature. According to the present model, this trend is calculated to be due to the decrease in quantity of ferric to ferrous ratio with temperature in air. Both the molar volumes from the linear model and the present model are similar in this composition range and can reproduce the temperature dependence. However, both models predict higher molar volume by approximately 5 pct. It was impossible to reproduce these experimental data without significantly sacrificing the accuracy of the model in higher order systems.

### C. Quaternary Systems

#### 1. MgO-CaO-FeO-Fe<sub>2</sub>O<sub>3</sub> system

This quaternary system was recently studied by Vadasz *et al.*<sup>[43]</sup> in air using the MBP method with nitrogen gas. The results are moderately well reproduced, as shown in Figure 9. However, it is noted that

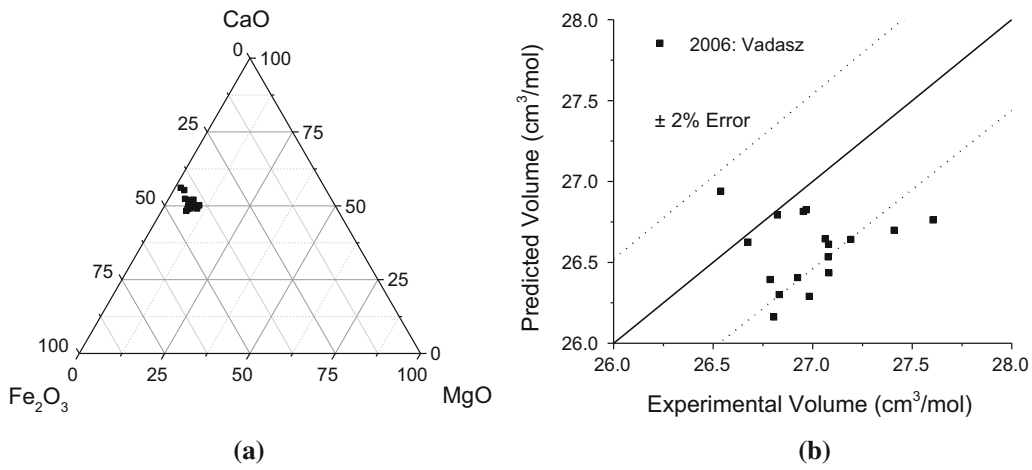


Fig. 9—The quaternary MgO-CaO-FeO-Fe<sub>2</sub>O<sub>3</sub> system in air: (a) compositions (mol pct) examined and (b) model accuracy.<sup>[43]</sup>

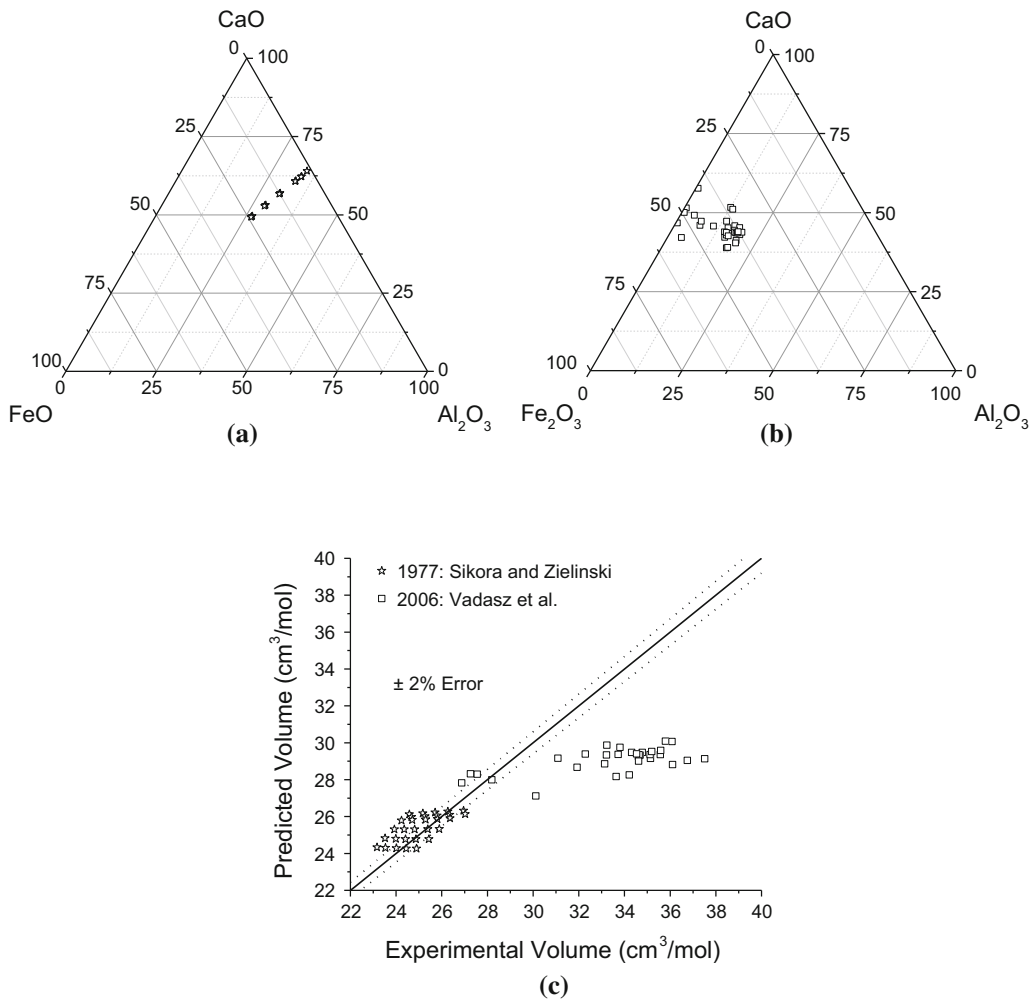


Fig. 10—The quaternary CaO-FeO-Fe<sub>2</sub>O<sub>3</sub>-Al<sub>2</sub>O<sub>3</sub> system: compositions (mol pct) examined (a) in iron saturation,<sup>[35]</sup> (b) in air,<sup>[36]</sup> and (c) accuracy of present model with 2 pct error limits (dotted lines).

the results of Vadasz *et al.* are considered to be less accurate because of MBP technique. Their results in the CaO-FeO-Fe<sub>2</sub>O<sub>3</sub> system are also less accurate compared

to the data obtained by DBA technique. Part of the measurements at 1623 K (1350 °C) are potentially below the liquidus.



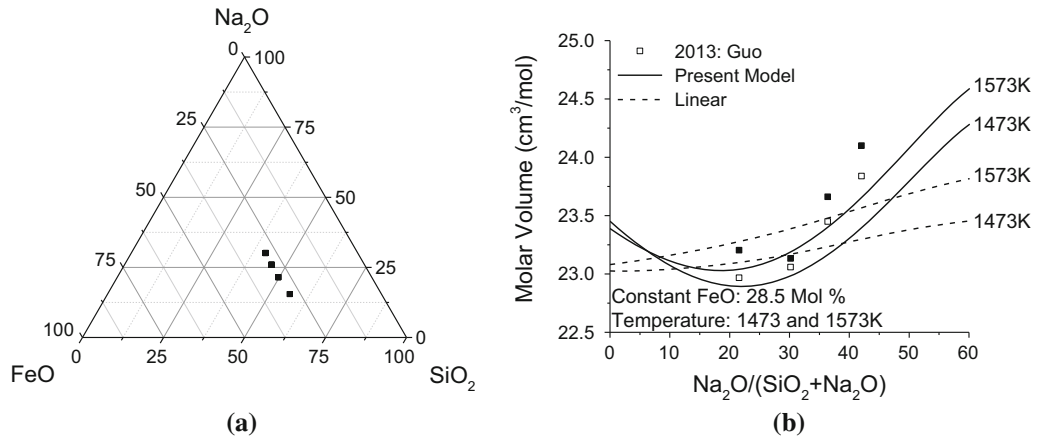


Fig. 11—The quaternary Na<sub>2</sub>O-FeO-Fe<sub>2</sub>O<sub>3</sub>-SiO<sub>2</sub> system in iron saturation: (a) compositions (mol pct) examined and (b) FeO = 28.5 mol pct iso-compositional section.<sup>[34]</sup> Filled symbols are at 1573 K (1300 °C) and opened symbols are at 1473 K (1200 °C).

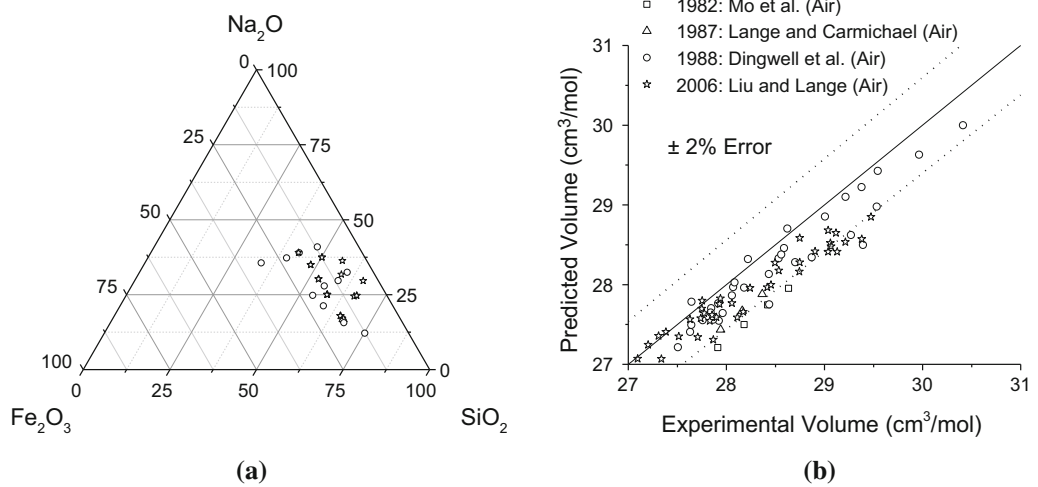


Fig. 12—The quaternary Na<sub>2</sub>O-FeO-Fe<sub>2</sub>O<sub>3</sub>-SiO<sub>2</sub> system in air: (a) compositions (mol pct) examined and (b) model accuracy.<sup>[29,31–33]</sup>

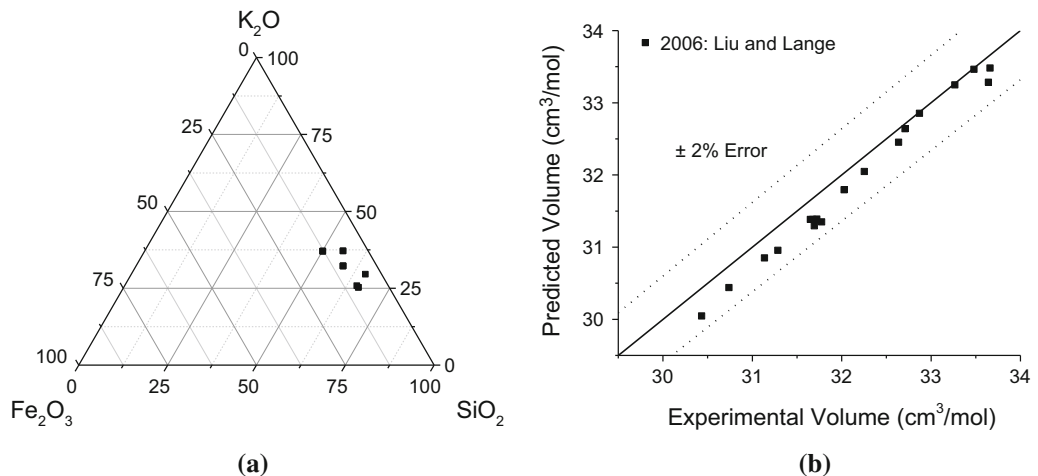


Fig. 13—The quaternary K<sub>2</sub>O-FeO-Fe<sub>2</sub>O<sub>3</sub>-SiO<sub>2</sub> system in air: (a) compositions (mol pct) examined and (b) model accuracy.<sup>[33]</sup>

## 2. CaO-FeO-Fe<sub>2</sub>O<sub>3</sub>-Al<sub>2</sub>O<sub>3</sub> system

This quaternary system in Fe saturation was examined by Sikora and Zielinski<sup>[35]</sup> using the MBP method

in a temperature range between 1723 K and 1923 K (1450 °C and 1650 °C) (Figure 10). They started with a CaO-Al<sub>2</sub>O<sub>3</sub> melt and added iron oxide. Their results in

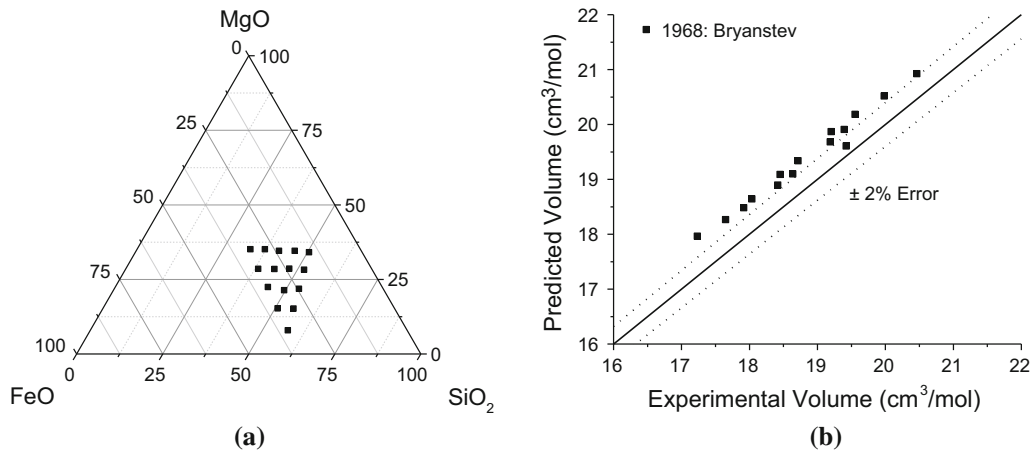


Fig. 14—The quaternary MgO-FeO-Fe<sub>2</sub>O<sub>3</sub>-SiO<sub>2</sub> system in iron saturation: (a) compositions (mol pct) examined and (b) model accuracy.<sup>[37]</sup>

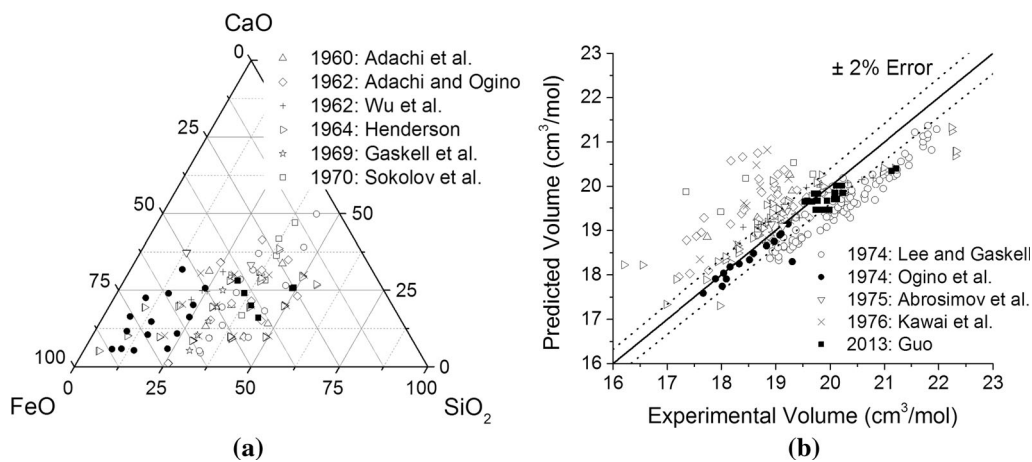


Fig. 15—The CaO-FeO-Fe<sub>2</sub>O<sub>3</sub>-SiO<sub>2</sub> system in iron saturation (approximated as the FeO-CaO-SiO<sub>2</sub> system).<sup>[14,18–21,24,26,27,34,38,39]</sup>

the CaO-Al<sub>2</sub>O<sub>3</sub> system suggested a very high thermal expansion and were inconsistent with other results (see Part I). Vadasz *et al.*<sup>[36]</sup> (MBP) examined several compositions in air at 1573 K (1300 °C). As seen in the previous CaO-MgO-FeO-Fe<sub>2</sub>O<sub>3</sub> system, their results are much higher than the predictions from both a linear model and the present model. In addition, based on the phase diagram calculated by FactSage, the experiments were carried out at sub-liquidus temperature.

### 3. Na<sub>2</sub>O-FeO-Fe<sub>2</sub>O<sub>3</sub>-SiO<sub>2</sub> system

*a. Iron saturation.* This quaternary system was examined by Guo<sup>[34]</sup> using a DBA technique using a 1 pct CO—99 pct Ar atmosphere. As the partial pressure of oxygen was sufficiently low, this study can be approximated as being in iron saturation. The compositions examined are along with the iso-FeO section ( $X_{\text{FeO}} = 0.285$ ) as shown in Figure 11. The experimental molar volume data show a non-linear trend (minimum at 20–30 mol pct of Na<sub>2</sub>O/(Na<sub>2</sub>O+SiO<sub>2</sub>)), which is

reasonably well predicted by the present model. This non-linear behavior is due to the increasing volume trend in the binary Na<sub>2</sub>O-SiO<sub>2</sub> system with the addition of Na<sub>2</sub>O and decreasing molar volume in the FeO-SiO<sub>2</sub> system in iron saturation. This will be discussed in more details in Section V.

*b. Air (Na<sub>2</sub>O-Fe<sub>2</sub>O<sub>3</sub>-SiO<sub>2</sub>).* This quaternary system in air was examined in four publications,<sup>[29,31–33]</sup> all of which used the DBA method. All the results are moderately well predicted with the present model leaning toward a slight under-prediction, as shown in Figure 12.

### 4. K<sub>2</sub>O-FeO-Fe<sub>2</sub>O<sub>3</sub>-SiO<sub>2</sub> System

This system was only examined in air by Liu and Lange<sup>[33]</sup> using the DBA method at temperatures between 1273 K and 1723 K (1000 °C and 1450 °C). The results are well predicted as shown in Figure 13. No research groups have examined this system in iron saturation.

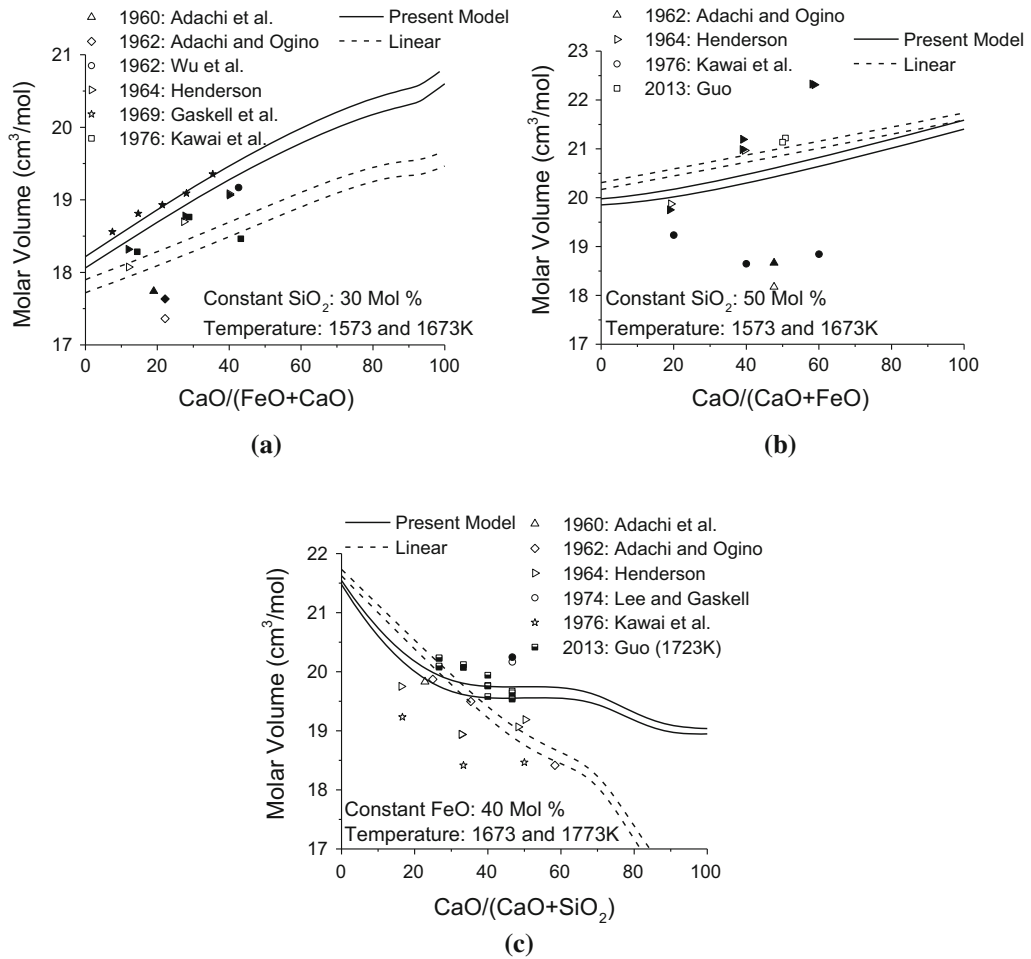


Fig. 16—The molar volume in the quaternary CaO-FeO-Fe<sub>2</sub>O<sub>3</sub>-SiO<sub>2</sub> system in iron saturation across the (a) SiO<sub>2</sub> = 30 mol pct,<sup>[14,21,26,27,38,39]</sup> (b) SiO<sub>2</sub> = 50 mol pct,<sup>[14,21,26,34]</sup> and (c) FeO = 40 mol pct<sup>[14,19,21,26,34,38,39]</sup> joins. Filled symbols are at 1673 K (1400 °C) and opened symbols are at 1573 K (1300 °C).

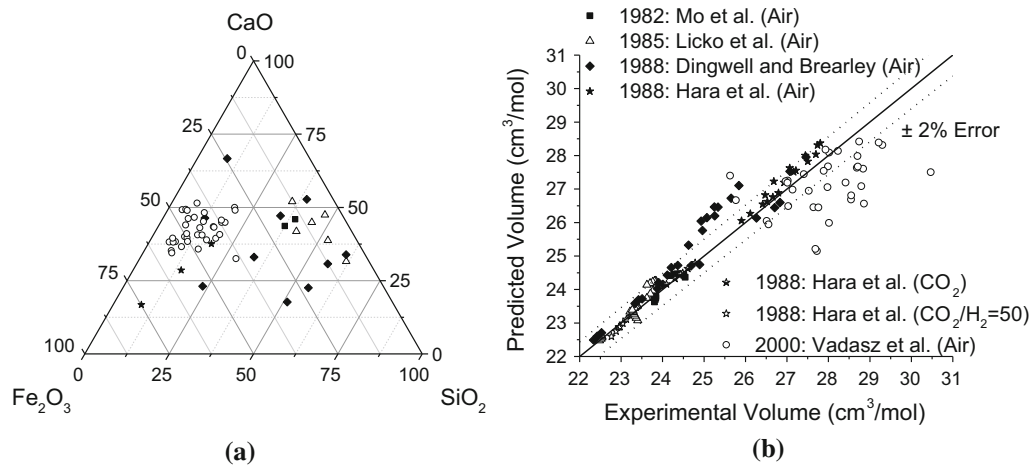


Fig. 17—The quaternary CaO-FeO-Fe<sub>2</sub>O<sub>3</sub>-SiO<sub>2</sub> system in air and other conditions: (a) compositions (mol pct) examined in air and (b) model accuracy.<sup>[23,29,36,40,41]</sup>

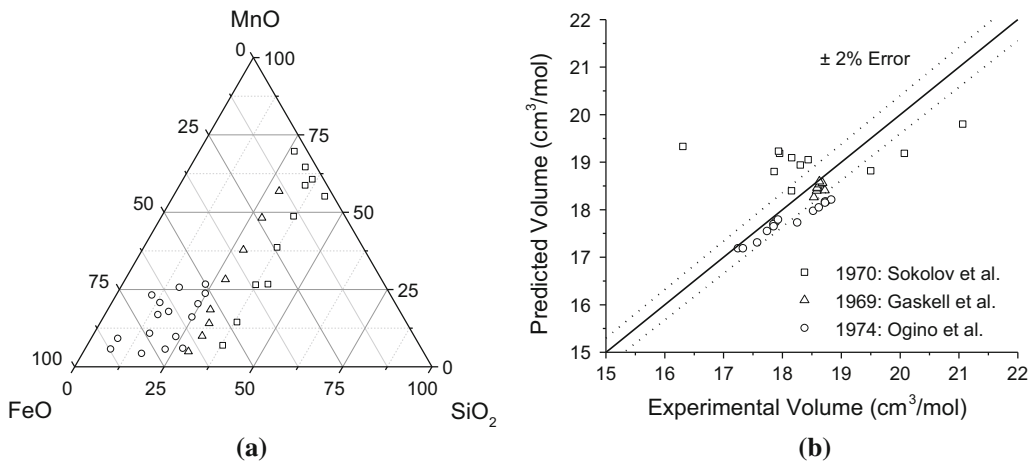


Fig. 18—The quaternary MnO-FeO-Fe<sub>2</sub>O<sub>3</sub>-SiO<sub>2</sub> system in iron saturation: (a) compositions (mol pct) examined and (b) model accuracy.<sup>[18,20,27]</sup>

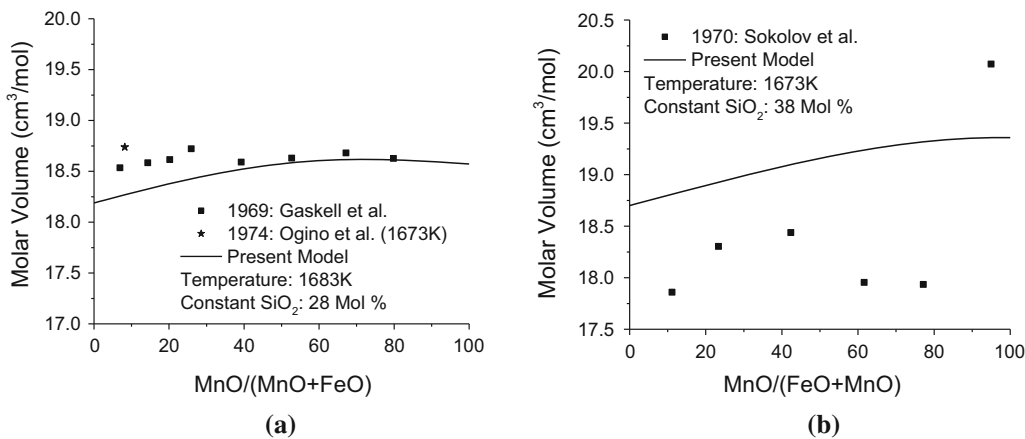


Fig. 19—The molar volume of the MnO-FeO-Fe<sub>2</sub>O<sub>3</sub>-SiO<sub>2</sub> quaternary system in iron saturation across the (a) SiO<sub>2</sub> = 28 mol pct<sup>[20,27]</sup> and (b) SiO<sub>2</sub> = 38 mol pct<sup>[18]</sup> binary joins.

### 5. MgO-FeO-Fe<sub>2</sub>O<sub>3</sub>-SiO<sub>2</sub> System

This quaternary system was examined by Bryanstev<sup>[37]</sup> using the MBP method in iron saturation (Figure 14). All measurements were performed at 1723 K (1450 °C). All the experimental results are systematically over predicted by approximately 2 pct, but the general trend is well predicted by the present model.

### 6. CaO-FeO-Fe<sub>2</sub>O<sub>3</sub>-SiO<sub>2</sub> System

*a. Iron saturation.* The CaO-FeO-Fe<sub>2</sub>O<sub>3</sub>-SiO<sub>2</sub> system in iron saturation, approximated as the CaO-FeO-SiO<sub>2</sub> system, was studied across wide compositions ranges as shown in Figure 15. The experimental data were measured using DBA<sup>[20,34]</sup> and MBP<sup>[14,18,19,21,24,26,27,38,39]</sup> techniques. In order to provide further insight into this system, binary sections are shown in Figure 16 across the 30 and 50 mol pct SiO<sub>2</sub> as well as the 40 mol pct FeO joins. The iso-SiO<sub>2</sub> joins provide insight into the effects of CaO and FeO substitution.

Along the 30 and 50 mol pct SiO<sub>2</sub> sections, the results of Gaskell *et al.*<sup>[27]</sup> (MBP) and Guo<sup>[34]</sup> (DBA) are well predicted. The remaining experimental data all obtained by MBP method suggest lower molar volumes and are very scattered.

The 40 mol pct FeO section was examined at multiple compositions by Guo<sup>[34]</sup> and their data are well predicted by the present model. The previous linear model also reasonably reproduces the molar volumes in this system. The large difference between two models in low SiO<sub>2</sub> is mainly due to the differences in molar volume for CaO.

*b. Air and other conditions.* This system was examined by several research groups in air; Mo *et al.*<sup>[29]</sup> (DBA), Licko *et al.*<sup>[40]</sup> (SBA), Dingwell and Brearley<sup>[41]</sup> (DBA), Hara *et al.*<sup>[23]</sup> (DBA), and Vadasz *et al.*<sup>[36]</sup> (MBP). In addition, Hara *et al.*<sup>[23]</sup> (DBA) also examined several compositions under CO<sub>2</sub> and CO<sub>2</sub>/H<sub>2</sub> = 50 atmospheres. All the compositions studied in air are shown in

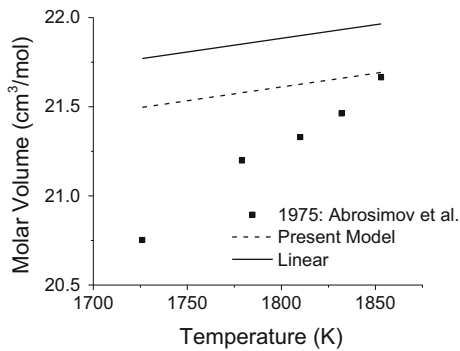


Fig. 20—Molar volume of a 45 FeO—47 SiO<sub>2</sub>—8 Al<sub>2</sub>O<sub>3</sub> melt (in mol pct) with iron saturation as a function of temperature.<sup>[24]</sup>

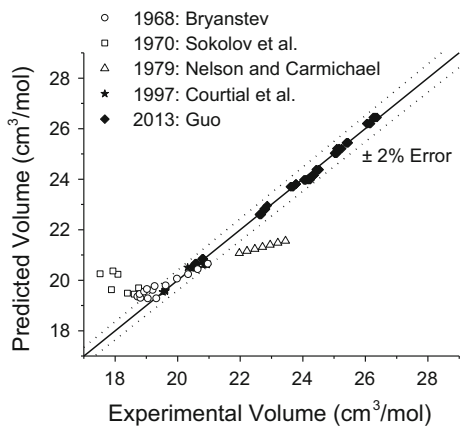


Fig. 21—Accuracy of the predictions of the present model in quinary and higher order iron oxide-containing systems.<sup>[18,29,30,34,37,42]</sup>

Figure 17(a) in addition to the accuracy of the model for predicting the experimental data in Figure 17(b) (including measurements not in air). The results of Mo *et al.* (DBA), Licko *et al.* (SBA), and Hara *et al.* (DBA) are all well predicted. Like other systems (CaO-FeO-Fe<sub>2</sub>O<sub>3</sub>-Al<sub>2</sub>O<sub>3</sub> and CaO-FeO-Fe<sub>2</sub>O<sub>3</sub>-MgO), the results of Vadasz *et al.* (MBP) are poorly reproduced. The results of Dingwell and Brearley are quite scattered, and some of their results are well reproduced while other are not. The composition measured by Dingwell and Brearley is located in the middle of the composition range studied by Vadasz *et al.* and their data are well predicted within 0.5 to 1 pct error.

#### 7. MnO-FeO-Fe<sub>2</sub>O<sub>3</sub>-SiO<sub>2</sub> System

The manganese-containing iron silicate system has only been studied in iron saturation. The compositions measured are shown in Figure 18 along with the accuracy of the model. Sokolov *et al.*<sup>[18]</sup> and Gaskell *et al.*<sup>[27]</sup> performed their experiments using the MBP method, while Ogino *et al.*<sup>[20]</sup> used the DBA method. To better illustrate some of the experimental data, the 28 and 38 mol pct SiO<sub>2</sub> sections are shown in Figure 19.

The results of Gaskell *et al.* and Ogino *et al.* are reasonably well predicted. However, the results of Sokolov *et al.* are very scattered.

#### 8. FeO-Fe<sub>2</sub>O<sub>3</sub>-Al<sub>2</sub>O<sub>3</sub>-SiO<sub>2</sub> system

A single composition of the FeO-Fe<sub>2</sub>O<sub>3</sub>-Al<sub>2</sub>O<sub>3</sub>-SiO<sub>2</sub> system with Fe saturation was examined by Abrosimov *et al.*<sup>[24]</sup> using the MBP method. The molar volumes of a 47 SiO<sub>2</sub>-8 Al<sub>2</sub>O<sub>3</sub>-45 FeO melt (in mol pct) at multiple temperatures are shown in Figure 20. Tomasek *et al.*<sup>[45]</sup> and Fadeev *et al.*<sup>[46]</sup> also examined the system using the MBP method, but it was not possible to obtain either of these results. They were referred in the review performed by Mills and Keene.<sup>[47]</sup>

#### D. Quinary and Higher Order Systems

Several higher order systems have been examined. However, it is difficult to illustrate the compositions studied graphically. The prediction accuracy of the model for the experimental data in higher order systems is shown in Figure 21. The most accurate data available are from of Courtial *et al.*<sup>[30]</sup> (DBA in the MgO-CaO-Al<sub>2</sub>O<sub>3</sub>-FeO<sub>x</sub>-SiO<sub>2</sub> system in air) and Guo *et al.*<sup>[34]</sup> (DBA in various systems under a 99 pct Ar—1 pct CO atmosphere) and they were well predicted by the present model. The data of Bryanstev<sup>[37]</sup> (MBP in the MgO-FeO<sub>x</sub>-SiO<sub>2</sub> system with Na<sub>2</sub>O, CaO, or Al<sub>2</sub>O<sub>3</sub> additions in iron saturation) and Sokolov *et al.*<sup>[18]</sup> (MBP in the CaO-MnO-FeO<sub>x</sub>-SiO<sub>2</sub> system in iron saturation) are less accurate. The data of Nelson and Carmichael<sup>[42]</sup> (DBA with a single composition in the CaO-Al<sub>2</sub>O<sub>3</sub>-FeO<sub>x</sub>-SiO<sub>2</sub> system in iron saturation) is uncertain as some of their results have been questioned in other systems.

## IV. DISCUSSIONS

#### A. Model and Experimental Data for Fe Oxide-Containing System

The present model for iron-containing systems provides a reasonable reproduction (typically within 2 pct error) of available reliable experimental data. Iron oxide-containing systems are less reproducible by linear models. Although the accurate data of Hara *et al.*<sup>[23]</sup> in the CaO-FeO-Fe<sub>2</sub>O<sub>3</sub> system are reproducible with a linear model, these parameters are not compatible with the parameters required to reproduce the molar volumes of silica-bearing melts. This suggests that a linear model cannot reproduce all the experimental data across the entire composition ranges and that non-linear terms are required. The non-linear behavior of molar volume with SiO<sub>2</sub> can be seen in the FeO<sub>x</sub>-SiO<sub>2</sub> system in iron saturation. The linear model of Lange and Carmichael<sup>[5]</sup> can reproduce the experimental data of geological melts containing a small amount of iron oxide, but its extrapolation to low silica region is poor.

There are various systems which require more information in order to better constrain molar volumes and

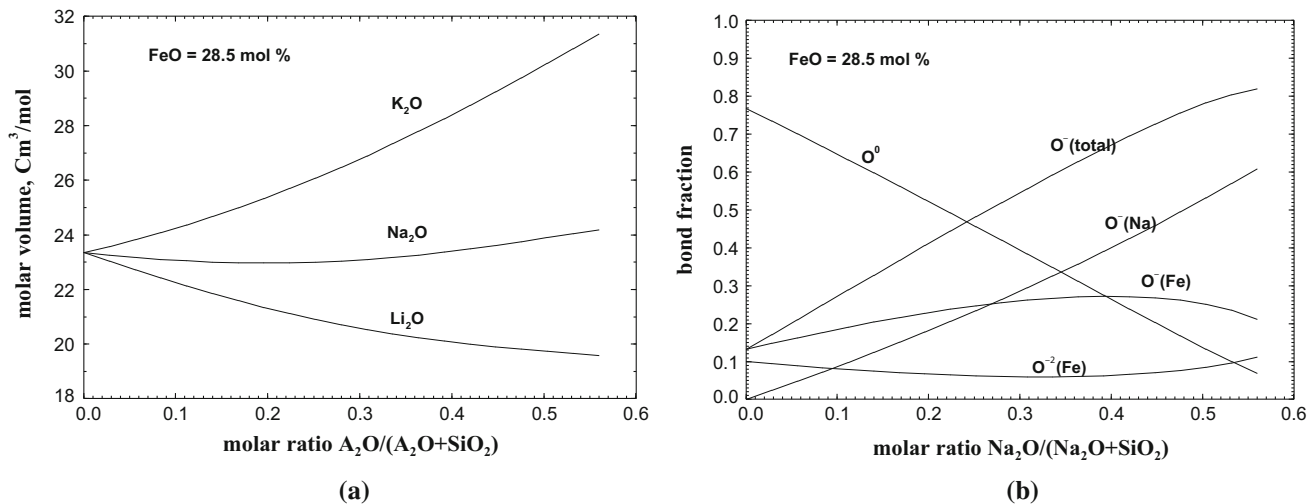


Fig. 22—(a) Predicted molar volume of  $A_2O$ -FeO-SiO<sub>2</sub> melt (A = Li, Na, and K) at 1573 K (1300 °C) and Fe saturation and (b) calculated bond fraction in the Na<sub>2</sub>O-FeO-SiO<sub>2</sub> melt at the same condition.

thermal expansions. In particular, even simple systems under oxidizing conditions have rarely been studied. In particular, the FeO<sub>x</sub>-SiO<sub>2</sub> system under oxidizing conditions (Fe<sub>2</sub>O<sub>3</sub>-SiO<sub>2</sub>) would aid greatly in optimizing the molar volume of Fe<sub>2</sub>O<sub>3</sub> and Fe<sub>2</sub>O<sub>3</sub>-SiO<sub>2</sub> system. In addition, the temperature dependence (thermal expansion) of most iron-bearing melts is relatively poorly studied.

### B. Molar Volume of Alkali Oxide-FeO-SiO<sub>2</sub> Melts

As can be seen in Figure 11, the molar volume of Na<sub>2</sub>O-FeO-SiO<sub>2</sub> melt in iron saturation (reducing atmosphere) clearly shows a non-linear behavior with the variation of Na<sub>2</sub>O/(Na<sub>2</sub>O + SiO<sub>2</sub>). In particular, a minimum in the molar volume is observed experimentally, which is well predicted by the present model. This behavior seems to result from the competitive contribution of Na and Fe to the molar volume of Q species.

Figure 22(a) shows the predicted molar volume of alkali oxide-SiO<sub>2</sub> with 28.5 mol pct FeO in iron saturation at 1573 K (1300 °C). The predicted molar volume for K<sub>2</sub>O- and Li<sub>2</sub>O-containing melts shows increasing and decreasing trend with A<sub>2</sub>O/(A<sub>2</sub>O + SiO<sub>2</sub>), respectively, where A = K or Li. On the other hand, the molar volume of Na<sub>2</sub>O-containing melt shows the minimum as discussed above. In order to examine the different trends in molar volume more clearly, the change in bond fraction in the alkali oxide-FeO-SiO<sub>2</sub> is calculated in Figure 22(b). Because the trend of the bond fraction was similar for all alkali oxide cases, only the results of Na<sub>2</sub>O-FeO-SiO<sub>2</sub> melt are plotted. At constant FeO concentrations, in general, the amount of broken oxygen bond increases with increasing amount of Na<sub>2</sub>O. In the low-Na<sub>2</sub>O region, the broken oxygen bonds are mostly caused by Fe, O<sup>-</sup>(Fe). Increasing Na<sub>2</sub>O in melt gradually increases the broken oxygen bonds, O<sup>-</sup>(Na). When the molar ratio of Na<sub>2</sub>O/(Na<sub>2</sub>O + SiO<sub>2</sub>) in the melt is higher than 0.27, the contribution of Na to the broken oxygen bond becomes larger than Fe. Similar trends in bond

fractions are also calculated for the melts containing K<sub>2</sub>O and Li<sub>2</sub>O.

In the presented molar volume model, molar volume is calculated based on the volume of individual Q<sup>n</sup> species. For ternary and multicomponent melt, the molar volume of Q<sup>n</sup> species is calculated considering the linear volume change between binary Q<sup>n</sup> species:

$$\text{molar volume of } Q^n \text{ species} = n_{Q^n} \frac{\sum_i x_{Si-i} (a_{ni} + b_{ni}T)}{\sum_i x_{Si-i}}, \quad [4]$$

where  $a_{ni} + b_{ni}T$  is binary molar volume parameter of Q<sup>n</sup> and  $x_{Si-i}$  is bond fraction of broken oxygen by *i* cation (for example, O<sup>-</sup>(Na) and O<sup>-</sup>(Fe) calculated in Figure 22). Therefore, the molar volume of binary Q<sup>n</sup> species and the amount of broken oxygen by each cation determine the molar volume in ternary and multicomponent systems.

In the case of Na<sub>2</sub>O-FeO-SiO<sub>2</sub> melt, the molar volume of ternary melt in Figure 22 is mainly calculated from the binary Na<sub>2</sub>O-SiO<sub>2</sub> and FeO-SiO<sub>2</sub>. At low Na<sub>2</sub>O concentration, the molar volume is primarily a function of the FeO-SiO<sub>2</sub> melt. As can be seen in Figures 5 and 6, the molar volume of FeO-SiO<sub>2</sub> melt decreases with decreasing SiO<sub>2</sub> content. The molar volume of Na<sub>2</sub>O-SiO<sub>2</sub> melt is almost constant between 0.0 and 0.2  $X_{Na_2O}$  and increases with increasing Na<sub>2</sub>O content. These two competitive contributions of Na<sub>2</sub>O and FeO result in the minimum in the molar volume of Na<sub>2</sub>O-FeO-SiO<sub>2</sub> melt as shown in Figure 22. However, in the case of K<sub>2</sub>O-FeO-SiO<sub>2</sub> melt, the molar volume increases continuously with increasing K<sub>2</sub>O because binary molar volume of K<sub>2</sub>O-SiO<sub>2</sub> increases sharply with increasing SiO<sub>2</sub> and the increasing rate of molar volume by the addition of K<sub>2</sub>O is higher than decreasing rate by FeO. The molar volume of Li<sub>2</sub>O-SiO<sub>2</sub> decreases with increasing Li<sub>2</sub>O content which results in a decreasing molar volume in the Li<sub>2</sub>O-FeO-SiO<sub>2</sub> melt.

A linear molar volume model cannot reproduce such non-linear molar volume behavior in the Na<sub>2</sub>O-FeO-SiO<sub>2</sub>

melt. Similar non-linear molar volume behavior can be expected in many ternary and multicomponent melts.

### C. General Discussion on Molar Volume Model and Future experimental Studies

The goal of this work was to fully examine the available literature on the molar volume of metallurgical slags and to obtain a non-linear melt structure-based model which can accurately reproduce molar volume in experimentally explored compositions and temperatures regimes, and to provide predictions in the unexplored regions. The molar volume of molten oxides should be related to their structure at a given composition and temperature. In the present work, the structural information was calculated from the Modified Quasichemical Model with optimized thermodynamic parameters. The model may be improved as more information on melt structure is made available to verify the Q-species amounts.

Based on the examination of the literature, there are wide composition ranges which have only been studied using relatively inadequate experimental techniques (e.g., systematic errors in SBA measurements, large errors in MBP measurements, and questionable imaging technique results) which promote the importance of modeling work based on the most accurate experimental data and systematic analysis. Previous modeling attempts of molar volume with linear models have focused primarily on silicate-rich melts. In the silica-rich region (>50 mol pct SiO<sub>2</sub>), a linear model is shown to provide accurate reproduction of the available experimental data and give reasonable predictions. A linear model is also mathematically simple to optimize and perform calculations. However, a growing quantity of experimental data in the low-SiO<sub>2</sub> region where most metallurgical slags are located suggests non-linear behavior of molar volume. This has been shown in various silicate systems such as the alkali binary silicates,<sup>[48,49]</sup> PbO-SiO<sub>2</sub>,<sup>[50,51]</sup> FeO-SiO<sub>2</sub>, CaO-Al<sub>2</sub>O<sub>3</sub>-SiO<sub>2</sub>,<sup>[52]</sup> and TiO<sub>2</sub>-bearing melts<sup>[53]</sup> (not examined in this work). The thorough examinations by Bottinga *et al.*<sup>[54-56]</sup> also suggests that linear models should only be applied between 0.35 and 0.85 mol fraction silica and non-linear terms should be introduced into the alumina-bearing systems. The present structure-based model can provide more accurate calculation of molar volume in the entire range of compositions.

## V. SUMMARY

A structural molar volume model was developed to accurately reproduce the molar volume of molten slags containing iron oxides under the oxygen partial pressures from metallic saturation to air. The experimental data for FeO-Fe<sub>2</sub>O<sub>3</sub>-Na<sub>2</sub>O-K<sub>2</sub>O-MgO-CaO-MnO-Al<sub>2</sub>O<sub>3</sub>-SiO<sub>2</sub> systems were critically reviewed and the unary and binary model parameters were optimized to reproduce the experimental data. The variation of ferric and ferrous iron oxides was taken carefully into account

during the review of the experimental data and molar volume modeling.

The present structural molar volume model can be used to calculate the molar volume of molten oxide in the Li<sub>2</sub>O-Na<sub>2</sub>O-K<sub>2</sub>O-MgO-CaO-MnO-PbO-FeO-Fe<sub>2</sub>O<sub>3</sub>-Al<sub>2</sub>O<sub>3</sub>-SiO<sub>2</sub> system across all ranges of compositions, temperature, and oxygen partial pressures under 1 atm total pressure. In future, the model and database can be further expanded to the systems containing Ti oxides, B<sub>2</sub>O<sub>3</sub>, and fluoride for a wider range of applications.

## ACKNOWLEDGMENTS

Financial support from Hyundai Steel, JFE Steel Corporation, Nippon Steel & Sumitomo Metal, Nucor Steel, Posco, RioTinto, RHI, RIST, Tata Steel Europe, Voestalpine, and the Natural Science and Engineering Research Council of Canada (NSERC) is gratefully acknowledged. One of the authors (E.T.) also acknowledges the scholarship from the Fonds de Recherche du Quebec - Nature et Technologies (FRQNT) supporting his master study.

## REFERENCES

1. E. Thibodeau, A.E. Gheribi, and I.-H. Jung: "Part I," accepted.
2. E. Thibodeau, A.E. Gheribi, and I.-H. Jung: "Part II," accepted.
3. A.D. Pelton and M. Blander: *Metall. Mater. Trans. B*, 1986, vol. 17B, pp. 805-15.
4. C.W. Bale, E. Bélisle, P. Chartrand, S.A. Decterov, G. Eriksson, K. Hack, I.H. Jung, Y.B. Kang, J. Melançon, A.D. Pelton, C. Robelin, and S. Petersen: *Calphad*, 2009, vol. 33, pp. 295-311.
5. R.L. Lange and I.S.E. Carmichael: *Rev. Min. Geochem.*, 1990, vol. 24, pp. 25-64.
6. S.A. Decterov, E. Jak, P.C. Hayes, and A.D. Pelton: *Metall. Mater. Trans. B*, 2001, vol. 32B, pp. 643-57.
7. E. Jak, P. Hayes, A. Pelton, and S. Decterov: *Int. J. Mater. Res.*, 2007, vol. 98, pp. 847-54.
8. I.-H. Jung, S.A. Decterov, and A.D. Pelton: *J. Phys. Chem. Solids*, 2004, vol. 65, pp. 1683-95.
9. S. Decterov, I. H. Jung, E. Jak, Y. B. Kang, P. Hayes, and A. Pelton: *VII International Conference on Molten Slags, Fluxes and Salts*, 2004, pp. 839-49.
10. I.-H. Jung, S.A. Decterov, and A.D. Pelton: *Metall. Mater. Trans. B*, 2004, vol. 35B, pp. 877-89.
11. Y. B. Kang and I. H. Jung: *VIII International Conference on Molten Slags, Fluxes and Salt*, 2009, pp. 459-71.
12. J. Henderson, R.G. Hudson, R.G. Ward, and G. Derge: *Trans. Am. Inst. Mining Metall. Pet. Eng.*, 1961, vol. 221, pp. 807-11.
13. A. Adachi, K. Ogino, and S. Kawasaki: *Technol. Rep. Osaka Univ.*, 1963, vol. 13, pp. 411-15.
14. J. Henderson: *Trans. Am. Inst. Mining Metall. Pet. Eng.*, 1964, vol. 230, pp. 501-04.
15. R.G. Ward and P.L. Sachdev: *Trans. Am. Inst. Mining Metall. Pet. Eng.*, 1965, vol. 233, pp. 1496-99.
16. D.R. Gaskell and R.G. Ward: *Trans. Metall. Soc. AIME*, 1967, vol. 239, pp. 249-52.
17. K. Mori and K. Suzuki: *Tetsu to Hagane*, 1968, vol. 54, pp. 1123-1127.
18. V.I. Sokolov, S.I. Popel, and O.A. Esin: *Izv. Vyssh. Uchebn. Zaved., Chern. Metall.*, 1970, vol. 13, pp. 10-15.
19. D.R. Gaskell and Y.E. Lee: *Metall. Trans.*, 1974, vol. 5, pp. 853-60.
20. K. Ogino, M. Hirano, and A. Adachi: *Technol. Rep. Osaka Univ.*, 1974, vol. 24, pp. 49-55.

21. Y. Kawai, K. Mori, H. Shiraishi, and N. Yamada: *Tetsu to Hagane*, 1976, vol. 62, pp. 53–61.
22. Y. Shiraishi, K. Ikeda, A. Tamura, and T. Saito: *Trans. Jpn. Inst. Met.*, 1978, vol. 19, pp. 264–74.
23. S. Hara, K. Irie, D.R. Gaskell, and K. Ogino: *Trans. Jpn. Inst. Met.*, 1988, vol. 29, pp. 977–89.
24. A. S. Abrosimov, E. G. Gavrin, and V. I. Ereimeichenkov, *Izvestiya Vysshikh Uchebnykh Zavedenii, Chernaya Metallurgiya*, 1975, pp. 14–17.
25. S. Sumita, K. Morinaga, and T. Yanagase: *J. Jpn. Inst. Met.*, 1983, vol. 47, pp. 127–31.
26. A. Adachi and K. Ogino: *Technol. Rep. Osaka Univ.*, 1962, vol. 12, pp. 147–52.
27. D.R. Gaskell, A. McLean, and R.G. Ward: *Trans. Faraday Soc.*, 1969, vol. 65, pp. 1498–508.
28. J. Holeczy, L. Bodnar, and K. Tomasek: *Hutn. Listy*, 1972, vol. 27, pp. 364–368.
29. X. Mo, I.S.E. Carmichael, M. Rivers, and J. Stebbins: *Min. Mag.*, 1982, vol. 45, pp. 237–45.
30. P. Courtial, E. Ohtani, and D.B. Dingwell: *Geochim. Cosmochim. Acta*, 1997, vol. 61, pp. 3111–19.
31. R.A. Lange and I.S.E. Carmichael: *Geochim. Cosmochim. Acta*, 1987, vol. 51, pp. 2931–46.
32. D.B. Dingwell, M. Brearley, and J.E. Dickinson, Jr: *Geochim. Cosmochim. Acta*, 1988, vol. 52, pp. 2467–75.
33. Q. Liu and R.A. Lange: *Am. Mineral.*, 2006, vol. 91, pp. 385–93.
34. X. Guo: Ph.D. Thesis, University of Michigan, 2013.
35. M. Zielinski and B. Sikora: *Prace Instytutu Metalurgii Zelaza im. Stanisława Staszica*, 1977, vol. 29, pp. 157–65.
36. P. Vadász, M. Havlík, and V. Daněk: *Can. Metall. Q.*, 2000, vol. 39, pp. 143–52.
37. B.A. Bryantsev: *Zhurnal Prikladnoi Khimii (Sankt-Peterburg, Russian Federation)*, 1968, vol. 41, pp. 2156–59.
38. A. Adachi, K. Ogino, and S. Kuno: *Tetsu to Hagane*, 1960, vol. 46, pp. 1243–44.
39. T.-F. Wu, A.F. Vishkarev, and V.I. Yavoiskii: *Izv. Vyssh. Uchebn. Zaved., Chern. Metall.*, 1962, vol. 5, pp. 66–75.
40. T. Licko, V. Danek, and Z. Panek: *Chem. Pap.*, 1985, vol. 39, pp. 599–605.
41. D.B. Dingwell and M. Brearley: *Geochim. Cosmochim. Acta*, 1988, vol. 52, pp. 2815–25.
42. S.A. Nelson and I.S.E. Carmichael: *Contrib. Miner. Petrol.*, 1979, vol. 71, pp. 117–24.
43. P. Vadász, M. Havlík, and V. Daněk: *Cent. Eur. J. Chem.*, 2006, vol. 4, pp. 174–93.
44. C. W. Thomas: Ph.D. Thesis, California Institute of Technology, 2013.
45. K. Tomasek, L. Bodnar, and J. Holeczy: *Hutn. Listy*, 1975, vol. 30, pp. 136–38.
46. O.N. Fadeev, I.F. Khudyakov, I.D. Kashcheev, and G.P. Kharitidi: *Izv. Vyssh. Uchebn. Zaved., Tsvetn. Metall.*, 1980, vol. 1, pp. 17–20.
47. K.C. Mills and B.J. Keene: *Int. Mater. Rev.*, 1987, vol. 32, pp. 1–120.
48. J.O.M. Bockris, J.W. Tomlinson, and J.L. White: *Trans. Faraday Soc.*, 1956, vol. 52, pp. 299–310.
49. J.W. Tomlinson, M.S.R. Heynes, and J.O.M. Bockris: *Trans. Faraday Soc.*, 1958, vol. 54, pp. 1822–33.
50. M. Hino, T. Ejima, and M. Kameda: *J. Jpn. Inst. Met.*, 1967, vol. 31, pp. 113–19.
51. H. Ito and T. Yanagase: *Trans. Jpn. Inst. Melts*, 1960, vol. 1, pp. 115–20.
52. P. Courtial and D.B. Dingwell: *Geochim. Cosmochim. Acta*, 1995, vol. 59, pp. 3685–95.
53. Q. Liu and R.A. Lange: *Geochim. Cosmochim. Acta*, 2001, vol. 65, pp. 2379–93.
54. Y. Bottinga and D.F. Weill: *Am. J. Sci.*, 1970, vol. 269, pp. 169–82.
55. Y. Bottinga, D. Weill, and P. Richet: *Geochim. Cosmochim. Acta*, 1982, vol. 46, pp. 909–19.
56. Y. Bottinga, P. Richet, and D.F. Weill: *Bull. Mineral.*, 1983, vol. 106, pp. 129–38.